The Sources of Parenchymal Regeneration After Chronic Hepatocellular Liver Injury in Mice

Pamela Vig,[1,2] Francesco P. Russo,[1] Robert J. Edwards,[3] Paul J. Tadrous,[2] Nicholas A. Wright,[2] Howard C. Thomas,[1] Malcolm R. Alison,[4] and Stuart J. Forbes[1]

After liver injury, parenchymal regeneration occurs through hepatocyte replication. However, during regenerative stress, oval cells (OCs) and small hepatocyte like progenitor cells (SHPCs) contribute to the process. We systematically studied the intra-hepatic and extra-hepatic sources of liver cell replacement in the hepatitis B surface antigen (HBsAg-tg) mouse model of chronic liver injury. Female HBsAg-tg mice received a bone marrow (BM) transplant from male HBsAg-negative mice, and half of these animals received retrorsine to block indigenous hepatocyte proliferation. Livers were examined 3 and 6 months post-BM transplantation for evidence of BM-derived hepatocytes, OCs, and SHPCs. In animals that did not receive retrorsine, parenchymal regeneration occurred through hepatocyte replication, and the BM very rarely contributed to hepatocyte regeneration. In mice receiving retrorsine, 4.8% of hepatocytes were Y chromosome positive at 3 months, but this was frequently attributable to cell fusion between indigenous hepatocytes and donor BM, and their frequency decreased to 1.6% by 6 months, as florid OC reactions and nodules of SHPCs developed. By analyzing serial sections and reconstructing a 3-dimensional map, continuous streams of OCs could be seen that surrounded and entered deep into the nodules of SHPCs, connecting directly with SHPCs, suggesting a conversion of OCs into SHPCs. In conclusion, during regenerative stress, the contribution to parenchymal regeneration from the BM is minor and frequently attributable to cell fusion. OCs and SHPCs are of intrinsic hepatic origin, and OCs can form SHPC nodules. (HEPATOLOGY 2006;43:316-324.)

After acute liver injury, parenchymal regeneration occurs through hepatocyte proliferation. However, under conditions of regenerative stress, bipotential oval cells (OCs) spread from the canals of Hering and can differentiate into hepatocytes.[1] A third potential compartment for liver regeneration is the bone marrow (BM). In normal mice, 1% to 2% of hepatocytes may be of BM origin[2]; however, others have found little or no contribution to the parenchyma from BM.[3] BM transplants have been used to correct a mouse model of tyrosinemia, a lethal hepatic enzyme deficiency. However, this occurs through fusion of BM-derived macrophages with the recipient's diseased hepatocytes.[4] The frequency of cell fusion has not yet been assessed with this unique model. Murine studies show BM–hepatocyte differentiation without cell fusion, but the magnitude has been small.[5,6]

Another potential regenerative cell is the small hepatocyte-like progenitor cell (SHPC). SHPCs share some phenotypes with hepatocytes, fetal hepatoblasts, and OCs, but are phenotypically distinct. They express markers such as albumin, transferrin, and alpha fetoprotein (AFP) and possess bile canaliculi and store glycogen. If rats are exposed to retrorsine (a pyrrolizidine alkaloid that is metabolized by the cytochrome P450 enzymes and prevents hepatocytes completing mitosis) before partial hepatectomy (PH), then liver mass is restored by the emergence and expansion of SHPCs.[7,8] The origin of SHPCs is debated. They may arise from a sub-population of hepato-

Abbreviations: OC, oval cells; BM, bone marrow; SHPC, small hepatocyte like progenitor cells; AFP, alpha-fetoprotein; PH, partial hepatectomy; HBsAg, hepatitis B surface antigen; PBS, phosphate-buffered saline; ISH, in situ hybridization; FITC, fluorescein isothiocyanate; SSC, standard sodium citrate; VRML, virtual reality modeling language; CK, cytokeratin.

From the [1]Hepatology Section, Imperial College London; the [2]Histopathology Laboratory, Cancer Research UK; the [3]Section of Experimental Medicine & Toxicology, Imperial College London; and the [4]Centre for Diabetes and Molecular Medicine, Queen Mary University of London, United Kingdom.

Received September 15, 2005; accepted November 2, 2005.

Address reprint requests to: Stuart J. Forbes, Department of Medicine, 10th Floor QEQM Building, Imperial College, St Mary's Campus, W2 1NY. E-mail: s.j.forbes@imperial.ac.uk; fax: (44) 207-886-1931.

Supported by The Wellcome Trust (Wellcome Project Grant awarded to M.R.A., Wellcome Advanced Fellowship awarded to S.J.F.), Cancer Research UK and The European Association for the Study of the Liver (Sheila Sherlock Fellowship awarded to F.P.R.).

Published online in Wiley InterScience (www.interscience.wiley.com).

DOI 10.1002/hep.21018

Potential conflict of interest: Nothing to report.

cytes that lack the necessary CYP enzyme for retrorsine metabolism and therefore escape its mitoinhibitory effects.[8] Evidence for a hepatocyte origin comes from experiments in rats in which mature hepatocytes were genetically labeled with an integrating transgene before PH and retrorsine exposure. This resulted in SHPCs containing the transgene replacing the liver parenchyma.[9] However, commentators have noted that the labeling technique may have labeled OCs or biliary epithelial cells, thereby not fully excluding these cells as a source of SHPCs.[10] Indeed, a subset of SHPCs have been shown to express OC markers OC.2 and OC.5.[7]

Here, we wished to study the extrahepatic and intrahepatic sources of liver regeneration in a model of a common chronic liver disease. We assessed the contribution to liver regeneration from extrahepatic (BM) and intrahepatic stem cells (OCs and SHPCs). In particular, we investigated the relationship between OCs and the SHPCs. To ascertain whether BM-derived cells contribute to liver regeneration, we examined the hepatitis B surface antigen (HBsAg) transgenic mouse model of chronic liver disease after a sex-mismatched BM transplant. To examine liver regeneration under "regenerative stress," we treated the HBsAg mice with retrorsine to block indigenous hepatocyte replication. In addition, we explored the intrahepatic formation of SHPC nodules by cutting serial sections through entire nodules, performing cytokeratin 8 and 18 immunostaining on these sections, digitally recording each image, and reconstructing 3-dimensional maps of nodules. This enabled the detection of cellular connections between structures such as the OCs and nodules of SHPCs that otherwise remain elusive when examining 2-dimensional figures.

Materials and Methods

Hepatitis B Surface Antigen Transgenic Mouse

All animal work was carried out under procedural guidelines and with ethical permission from the Home Office (UK). The HBsAg-tg transgenic mouse model of hepatitis B with chronic liver damage was used (TgN [Alb1HBV]44Bri from JAX Labs, Nar Harbor, ME).[11] These mice express the HBV BgIII-A fragment under the control of an albumin promoter, and nearly all of their hepatocytes are positive for HBsAg. This leads to the phenotype of ground glass hepatocytes, hepatocyte necrosis, and persistent regeneration with a bromodeoxyuridine-labeling index of 1% to 2%. There is a non-immune inflammatory hepatitis with the formation of dysplastic nodules and eventually liver cancer.

Bone Marrow Transplantation/Adoptive Transfer

Twenty-six–week old HBsAg-positive female recipient mice underwent whole-body gamma irradiation with 10 Gray in a divided dose 3 hours apart to ablate their BM followed immediately by a tail vein injection with whole male BM [1×10^6 cells in 200 μL phosphate-buffered saline (PBS)] from C57Black/J6 donor mice. BM was flushed from the femurs of the male donors with PBS, filtered through a 70-μm tube filter, and centrifuged at 400*g* for 5 minutes, then filtered and centrifuged as before then re-suspended in PBS for injection.

Retrorsine Treatment to Block Hepatocyte Regeneration

Retrorsine is a pyrrolizidine alkaloid metabolized by the cytochrome P450 mixed-function oxidases, which causes a long-lasting inhibition of resident hepatocyte proliferation.[12] Six weeks after BM transplantation, half of the animals were given 2 retrorsine injections 2 weeks apart. A dose of 70 mg/kg body weight was injected intraperitoneally. Retrorsine (Sigma-Aldrich, Poole, UK) was added to demineralized water, the pH adjusted to 2.0 to 2.5 to allow dissolution, neutralized to pH 7.2 with 1 mol/L NaOH, and NaCl was added to obtain a final concentration of 150 mmol/L. Animals were sacrificed at 3 and 6 months after BM transplant, and their livers were analyzed.

Immunohistochemical Analysis and Y Chromosome Detection

To identify the origin of cells in the liver, immunohistochemistry was combined with *in situ* hybridization (ISH) for the Y chromosome.

Immunohistochemistry

To identify hepatocytes in mouse liver sections, we immunostained for several hepatocyte markers: CK 8/18, albumin, CYP1A2 and alpha-fetoprotein, along with 2 markers of cell proliferation, Ki-67 (MIB-5) and MCM-2 and for CD45 (leukocyte common antigen). To identify indigenous hepatocytes, we immunostained for HBsAg. Four-μm-thick formalin-fixed paraffin wax–embedded sections were incubated with hydrogen peroxide (2.4 mL 30%) in methanol (400 mL) to block endogenous peroxidases. Antigen retrieval was performed by microwaving in sodium citrate or by trypsinization. Liver sections were treated with an avidin/biotin kit (DAKO, Cambridgeshire, UK; X0590), blocked in serum (either normal swine, goat, or rabbit serum diluted 1/25 in PBS; DAKO; catalogue nos. X0901, X0907, X0902) for 15 minutes, and then incubated in the primary antibody at an appropriate dilution for 35 minutes (see Table 1 for

Table 1. Details of Antibodies Used

Primary Antibody	Dilution	Secondary Antibody	Dilution	Manufacturer
CK 8/18 (rat polyclonal)	Neat	Rabbit anti-rat	1/100	Made in house at Cancer Research UK
HBsAg(goat polyclonal)	1/1000	Rabbit anti-goat	1/100	DAKO, Cambridgeshire, UK B0560
CD45 (rat polyclonal)	1/10	Rabbit anti-rat	1/100	BD Pharmingen, San Diego, CA
Albumin (rabbit polyclonal)	1/800	Swine anti-rabbit	1/500	DAKO, Cambs. UK A0001
CYP 1A2 (rabbit polyclonal)	1/200	Swine anti-rabbit	1/500	Gift from Dr. Robert Edwards, Imperial College, Hammersmith Campus, London, UK
Alpha-fetoprotein (goat polyclonal)	1/25	Rabbit anti-goat	1/100	Santa Cruz Biotechnology, Santa Cruz, CA, USA SC8108
Ki-67/MIB 5 (rabbit polyclonal)	1/200	Swine anti-rabbit	1/500	Novocastra, Newcastle, UK NCL-Ki67p
MCM 2 (mouse monoclonal)	Neat	Rabbit anti-mouse	1/300	Gift from Dr. Steven Dilworth, Imperial College, Hammersmith Campus, London, UK

details). A biotinylated secondary antibody (see Table 1) was then applied for 35 minutes. If the sections were carried through for ISH, then a tertiary layer of streptavidin-alkaline phosphatase (DAKO; D0396) diluted to 1/50 in PBS was applied for 35 minutes followed by PBS washes and development with Vector Red (Vector Laboratories, Peterborough, UK; SK5100). Alternatively, a layer of streptavidin-horseradish peroxidase (DAKO; P0397) diluted to 1/500 in PBS for 35 minutes was applied, followed by PBS washes and a 2-minute incubation in 3,3′-diaminobenzidine (0.005 g in 10 mL PBS). Sections were washed in PBS before the ISH protocol.

In Situ *Hybridization*

Sections were incubated in 1 mol/L sodium thiocyanate for 10 minutes at 80°C, washed in PBS, then digested in pepsin (0.4% w/v) in 0.1 mol/L HCl at 37°C for 5 to 10 minutes. The protease was quenched in glycine (0.2% v/w) in 2× PBS, post-fixed in paraformaldehyde (4% w/v) in PBS, dehydrated through graded alcohols then air-dried. A fluorescein isothiocyanate (FITC)-labeled Y-chromosome paint (Star-FISH, Cambio, Cambridge, UK, Cat. No. 1189-YMF-01) was added to the sections, sealed under glass with rubber cement, heated to 80°C for 10 minutes, and then incubated overnight at 37°C. The slides were washed in formamide (50% w/v)/2× saline sodium citrate (SSC) at 37°C, then washed with 2× SSC, then washed with 4× SSC/Tween-20 (0.05% w/v) at 37°C. The slides were rinsed in 0.5× SSC at 37°C, then PBS before mounting in DAPI/Citifluor (Citifluor Ltd, London, UK), except for the sections that were double immunostained with the cy5-labeled antibody; in these the DAPI was omitted.

Microscopy and Image Capture

For light microscopy, a Nikon (Tokyo, Japan) Eclipse E600 microscope was used with a DXM 1200F digital camera. For fluorescent microscopy, slides were visualized using a Zeiss (Oberkochen, Germany) Axioplan 2 fluorescence microscope equipped with a triple-bandpass filter. Grayscale images were collected with a cooled charge-coupled device camera (Quantix Corp., New York, NY) and analyzed using Mastercapture software. For confocal microscopy, a Zeiss Axiovert 200 M microscope equipped with a triple bandpass filter was used; images were collected with CCD camera (Hall 100), analyzed with Zeiss LSM Image Browser software. Image processing used Adobe (San Jose, CA) Photoshop software.

Cell Counting

For cell counting in tissue processed for direct ISH, 20 consecutive frames (×40 objective) per slide (per animal) were digitally photographed under fluorescence microscopy, and then quantified from the digital images. The criteria for identification of a hepatocyte was a circular nuclear profile with a circumferential coating of cytokeratin 8/18 positive cytoplasm. In all tissue analysis, a male control liver and a female control liver were used. In addition, when quantifying cells, a calculated adjustment was made because in the male controls the Y chromosome could not be detected in all hepatocytes. In age-matched male controls, the number of hepatocytes containing the Y chromosome was 90%, and so the observed counts were divided by 0.9 to give actual numbers of bone marrow–derived cells. Results presented below are the corrected counts.

Three-Dimensional Modeling

Using software that allows interactive visualization, measurements, and segmentation, a 3-dimensional model was constructed to study the nodules of SHPCs that developed in the retrorsine-treated HBsAg transgenic mice. One hundred serial sections of a retrorsine-treated liver were cut and placed on slides. Immunohistochemistry for CK 8 and 18 was used to detect OCs, biliary epithelial cells, and hepatocytes in and surrounding the nodule. One nodule was serially photographed through 100 sections at a resolution of 300 pixels/inch. Images were ma-

nipulated by tracing bile ducts (green), portal veins (blue), central veins (turquoise), and OCs (pink) to study the relationship between these structures. The traced digital images were finely registered (aligned relative to each other) using freely available automated histological tissue section image registration software (Autoreg).[13] The 3-dimensional models were generated as fully manipulatable semi-transparent VRML (virtual reality modeling language) models using freely available 3D rendering sofware (FATCAM).[13] Using these models, one can make out the spatial relationship of these structures, (*i.e.,* OCs, bile ducts, portal veins) to the nodule.

Results

HBsAg-tg Model of Liver Damage in the Absence of Retrorsine

In the absence of retrorsine, a low-level hepatocyte regeneration occurred through indigenous hepatocyte replication. No OC reactions or nodules of SHPCs were identified, and by using ISH for the Y chromosome to detect cells of donor origin, we found that BM cells very rarely contribute to hepatocytes. Only 0.37% (range, 0.2-0.4; n = 5) of CK8/18 positive hepatocytes were Y chromosome positive at 3 months after the BM transplant, and 0.33% (range, 0.0%-0.5%, n = 5) at 6 months.

HBsAg-tg Model of Liver Damage Treated With Retrorsine

BM-Derived Liver Cells. Male and female control livers were used to confirm detection of the Y-chromosome using ISH (Fig. 1A-B). Many of the Y chromosome–positive cells in the recipient female mice were CD45 immunopositive, but many were not, suggesting non-hematopoietic differentiation (Fig. 1C). In the 3-month retrorsine-treated group, 4.7% (range, 1.3%-6.3%, n = 5) of CK 8/18-positive hepatocytes were Y chromosome positive (Fig. 1D and Table 2). At 6 months however, the number of Y-chromosome–positive hepatocytes dropped to 1.6% (range, 0%-3.4%, n = 5).

When the ISH protocol was combined with immunostaining for HBsAg, we found the percentage of HBsAg-positive and Y-positive hepatocytes was 2.59% (range, 2.0%-2.6%, n = 5) in the 3-month retrorsine-treated animals (Fig. 1E) and 0.63% (range, 0%-1.1%, n = 5) in the 6-month retrorsine-treated animals. By contrast, there was only 0.48% (range, 0.3%-0.6%, n = 5) and 0.52% (range, 0.4%-0.5%, n = 5) of HBsAg- and Y-positive hepatocytes in the 3-month and 6-month control groups, respectively (Table 2). Because the male BM was from mice that were not transgenic for HBsAg, hepatocytes arising through transdifferentiation should be HBsAg-negative and Y chromosome–positive. These findings

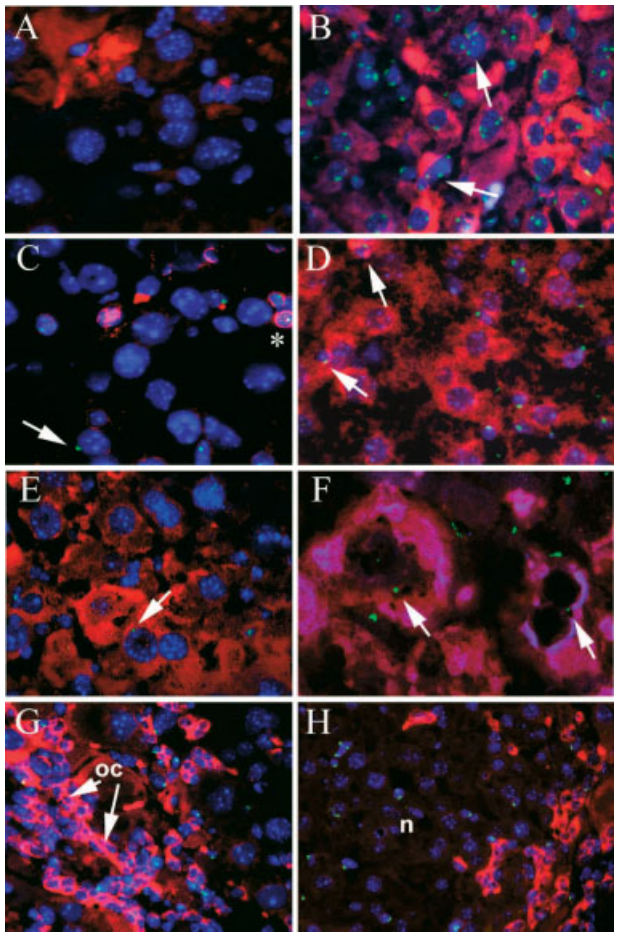

Fig. 1. Photomicrographs illustrating (A) female and (B) male control mouse livers demonstrating that the FITC-labeled Y-chromosome probe (fluorescent green) does not label female (XX) cells but labels male (XY) cells in the nucleus. (C-F) Parenchymal regions in female HBsAg-tg mice that received lethal irradiation at 6 weeks of age (10 Gray in divided doses) followed by BM transplant with 1×10^6 male BM cells. Six weeks after the BM transplantation, retrorsine (70 mg/kg body weight intraperitoneally) was injected on 2 occasions 2 weeks apart. Animals were killed at 3 or 6 months after BM transplantation. In images C-F, animals were killed at 3 months after BM transplantation. (C) In the liver, frequent Y-positive cells (fluorescent green signals) are CD45 positive (asterisk), but others are CD45 negative (arrow), suggesting non-hematopoietic differentiation. (D) Occasional CK8/18-positive (red) hepatocytes are Y-chromosome positive (arrows). (E) Confocal image of a 10-μm-thick section demonstrating that some of the HBsAg-positive hepatocytes (red) were Y chromosome positive (fluorescent green dot, arrow), suggesting possible cell fusion. (F) Confocal image of a 10-μm-thick section with triple labeling: HBsAg (blue), CK 8/18 (red) combined with FISH for Y detection (fluorescent green dot). Binucleate Y-chromosome–positive cells can be seen that are both CK 8/18 and HBsAg positive, suggestive of fusion between male BM cells and indigenous HBsAg-positive hepatocytes (arrows). (G) At 6 months after BM transplantation, cords of highly CK 8/18–immunopositive oval cells (OC) are evident that are largely Y chromosome negative. The few Y-chromosome–positive cells seen are adjacent to OCs but are not convincingly CK positive. (H) A nodule (n) of SHPCs at 6 months after BM transplantation, distinguished by small, round, uniformly sized nuclei. The SHPCs in the nodule are Y chromosome negative, with a few non-parenchymal Y-positive cells seen in the sinusoids. The nodules are always adjacent to an OC reaction. FITC, fluorescein isothiocyanate; HBsAg, hepatitis B surface antigen; BM, bone marrow.

Table 2. Properties of Y-Chromosome–Positive Hepatocytes

Treatment Group	CK 8/18 $^{+}$ Y^{+} Hepatocytes (%)	$HBsAg^{+}$ Y^{+} Hepatocytes (%)
3 months post BM transplantation no retrorsine	0.37 (range, 0.2-0.4)[a]	0.48 (range, 0.3-0.6)
3 months post BM transplantation with retrorsine	4.74 (range, 1.3-6.3)[a,b]	2.59 (range, 2.0-2.6)
6 months post BM transplantation no retrorsine	0.33 (range, 0.0-0.5)	0.52 (range, 0.4-0.5)
6 months post BM transplantation with retrorsine	1.58 (range, 0-3.4)[b]	0.63 (range, 0-1.1)

[a] $P < .05$ between the 3-month control group and the 3-month retrorsine-treated group
[b] $P < .05$ between the 3-month retrorsine-treated group and the 6-month retrorsine-treated group.

suggest that approximately half of the Y chromosome–positive cells are a result of cell fusion, where the indigenous female HBsAg-positive cell fuses with the male HBsAg-negative cell, hence the Y-positive, HBsAg-positive phenotype. To further understand and confirm this phenomenon, double immunohistochemical staining for HBsAg and CK 8/18 was combined with ISH. If the cell is HBsAg positive, it is originating from the resident liver, and if it is also cytokeratin (CK) positive, it is an HBsAg-positive hepatocyte. Moreover, if the same cell is marked with a Y-chromosome, this would demonstrate that cell fusion is occurring with hepatocytes. Sections were observed using confocal microscopy to give 3-dimensional images of thicker tissue sections. Results were consistent with cell fusion in some cells showing this triple staining (Fig. 1F).

Oval Cells. Three months after the BM transplantation, we could not identify any areas of OC activation; however, by 6 months OCs were abundant. We analyzed these areas for evidence of engraftment from the BM. Although frequent Y chromosome signals were seen close to areas of OC activation, none of the OCs were convincingly Y chromosome positive (Fig. 1G). However, these OC reactions were almost always directly abutting nodules of SHPCs that were also Y-chromosome negative (Fig. 1H). Because both the nodules and the OCs are Y chromosome negative, it is obvious that these SHPCs are not derived from the BM.

Nodules of SHPCs. With the emergence of the nodules at the 6-month point, the percentage of BM engraftment decreased. Fewer "BM-derived" hepatocytes were seen at 6 months than at 3 months, and the morphology of the liver was very different from that of the 3-month livers. At 6 months, there were large hepatocytes (megalocytes) surrounding frequent nodules of SHPCs (Fig. 2A-B). Nodules were largely CK 8,18 negative (Fig. 2C). Some of these nodules expressed HBsAg (Fig. 2D), whereas others were HBsAg negative (not shown). Immunohistochemistry for CK 8/18 combined with ISH showed that these SHPCs within the nodules were Y-chromosome negative, that is, they were not BM derived. The cells within the nodules were found to have characteristics of both mature hepatocytes and fetal hepatoblasts. They were albumin positive (Fig. 2E), AFP positive (Fig. 2F), but negative for CYP1A2 (Fig. 2G). The lack of CYP expression suggests that these cells may be arising from hepatocytes that lack the appropriate P450 enzymes to metabolize retrorsine and thus may escape its mitoinhibitory effects, resulting in proliferation of these cells. These SHPCs were previously described in retrorsine-treated rats that had been partially hepatectomized.[8] Whether these cells have malignant potential over time is not clear, but characterization of proliferation showed that 12.0% (range, 9.8%-15.0%, n = 4 as one was not evaluable) of SHPCs were Ki-67 positive (Fig. 2H) compared with 0.2% of hepatocytes without the nodules. The mitotic index was found to be 1.6% (range, 1.0%-2.1%, n = 4). Immunohistochemical staining for MCM-2 revealed 14.8% (range, 9.0%-17.0%, n = 4) of SHPCs within nodules were positive (Fig. 2I) compared with 0.7% of hepatocytes without the nodules (Table 3). The similarity between the 2 labeling indices suggests that these SHPCs are not dysplastic at this time.

Relationship of Oval Cells to SHPCs. One can see in Fig. 3A that the OCs within the nodule are frequently adjacent to SHPCs that are weakly cytokeratin 8/18 positive; however, in 2-dimensional images one cannot ascertain the 3-dimensional structure and cell relationships. To accurately determine the relationship between OCs and nodules of SHPCs, a 3-dimensional model was reconstructed from serial sections that were stained with CK 8/18 (Figs. 3, 4). This showed that streams of OCs were invariably surrounding the nodule and frequent lines of OCs penetrated the nodule at multiple sites (Fig. 3). Within a single nodule, multiple lines of OCs penetrate the nodules, directly connecting the portal tracts with "buds" of SHPCs. As lines of OCs are followed from the portal tract into the nodule, they connect directly with CK 8/18–positive SHPCs and intermingle with the CK 8/18–negative SHPCs (Fig. 4).

Discussion

We have investigated the contribution of extrahepatic and intrahepatic cells to liver regeneration after chronic liver injury both with and without retrorsine. We found

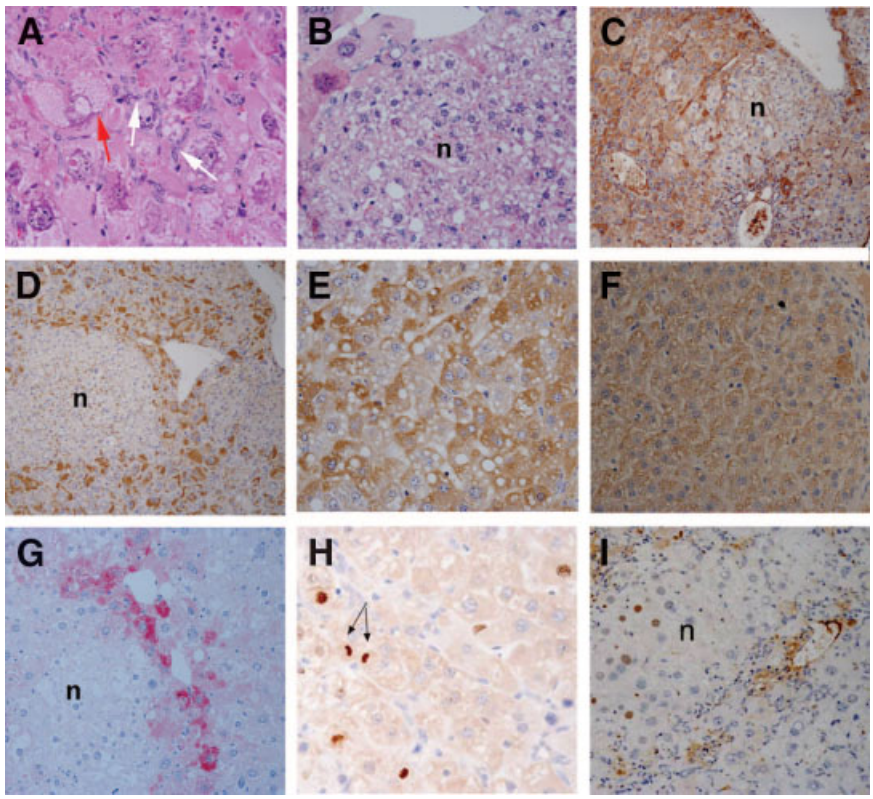

Fig. 2. Photomicrographs illustrating liver pathology at 6 months after BM transplantation. (A, B) Hematoxylin-eosin–stained sections. (A) Typical large hepatocytes/megalocytes (red arrow) with intermingled OCs (white arrows), (B) a nodule (n) of SHPCs surrounded by megalocytes. (C-I) Immunohistochemistry demonstrated that SHPCs were: (C) weakly CK 8/18 positive (brown), (D) often HBsAg-positive, (E) albumin positive, (F) AFP positive, (G) cytochrome P450 (CYP 1A2) negative, (H) containing Ki-67–positive cells (note the presence of the labeled SHPC in telophase, arrows), and (I) MCM-2–positive cells. BM, bone marrow; SHPC, small hepatocyte-like progenitor cells; OC, oval cell; HBsAg, hepatitis B surface antigen; AFP, alpha-fetoprotein.

that the contribution to liver regeneration from BM-derived cells was small, even when hepatocyte regeneration was inhibited by retrorsine, with only 4.7% of hepatocytes being Y chromosome positive at 3 months after BM transplantation. Furthermore, these cells had no selective advantage, as the level of BM-derived cells actually dropped to 1.6% at 6 months. Approximately half of the Y-positive hepatocytes were also positive for HBsAg, indicating fusion of the donor BM–derived cells with recipient hepatocytes. This decrease in the percentage of BM-derived hepatocytes may reflect the fact that the fusion cells are still abnormal and that regeneration is now provided by the OCs and SHPCs. This is broadly consistent with other rodent models of liver injury, and studies of human liver allografts that have not found evidence of large-scale BM-hepatocyte differentiation.[14] The initial increase in BM cell engraftment (0.37% vs. 4.7%), after retrorsine was presumably because the retrorsine inhibited replication of indigenous hepatocytes but not BM-derived hepatocytes that developed after retrorsine exposure. The BM stem cell chemokine SDF-1 may have a role in this effect; in rats given carbon tetrachloride, SDF-1 is upregulated only when animals are additionally exposed to 2-acetylaminofluorine to block hepatocyte replication.[15]

In the absence of retrorsine, parenchymal replacement occurs through hepatocyte replication as evidenced by the lack of an OC reaction or development of nodules of SHPCs. Mice that had been exposed to retrorsine for 6 months had a widespread OC reaction coincident with the appearance of numerous nodules of SHPCs. These SHPCs are immunopositive for albumin and AFP, had

Table 3. Proliferation Inside and Outside the Nodules of SHPCs at 6 Months Post BMT: Ki-67 and MCM-2

N = 4	Ki-67–Positive Hepatocytes (%)	Mitotic Index (%)	MCM-2–Positive Hepatocytes (%)
Within nodules of SHPCs	12.0% (range, 9.8-15.0)	1.6% (range, 1.0-2.1)	14.8% (range, 9.0-17.0)
Outside nodules of SHPCs	0.2% (range, 0.0-0.3)	0.0	0.7% (range, 0.4-0.9)

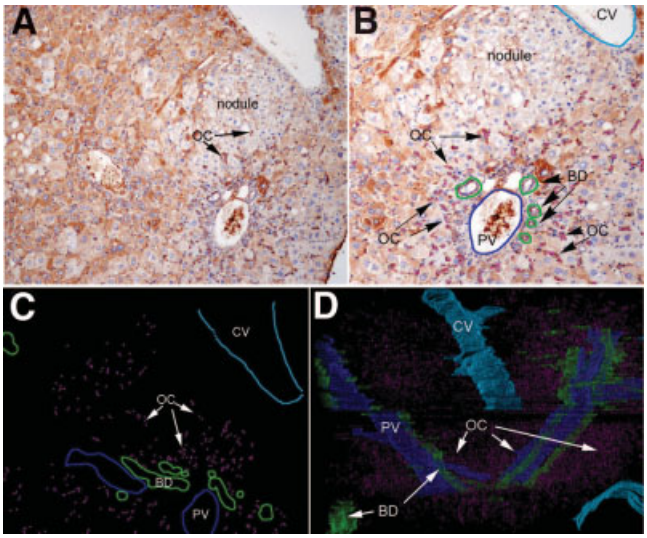

Fig. 3. Photomicrograph illustrating (A) an example of the nodule selected for 3-dimensional reconstruction. The nodule boundaries are visible by the CK staining that surrounds the nodule. Cytokeratin-dense OCs can be seen surrounding and within the nodule. (B) Construction of a 3-dimensional image with special attention to the relationship of OCs to the nodules of SHPCs. Bile ducts (BD) are traced in green, OCs are numerous around the nodule (OC), and are marked with pink dots, portal veins (PV) are traced in blue, and the central vein (CV) is traced in turquoise. The registration of the serial sections was then conducted to ensure that the images were aligned with one another to construct the 3-dimensional model. (C) A tracing without the original immunostained image for fine registration purposes, showing the spatial orientation of the structures. (D) A composite 3-dimensional model showing each structure (PV, BD, CV), with OCs originating from bile ducts surrounding and penetrating the region of the nodule. CK, cytokeratin; OC, oval cell; SHPC, small hepatocyte-like progenitor cells.

weak or absent CK8/18 expression, and were negative for CYP1A2. The lack of mixed-function oxidases may explain why, in the presence of retrorsine, such nodules expand and repopulate the liver. The nodules were proliferating with high labeling indices for cell cycle markers Ki-67 and MCM-2 compared with the replicative senescent hepatocytes without the nodule.

The potential lineage relationship between OCs, SHPCs, and hepatocytes has been unclear. SHPCs have been suggested to arise from a pre-existing retrorsine-resistant hepatocyte population lacking the appropriate cytochrome P450 enzymes. To address whether mature hepatocytes could give rise to SHPCs, Avril et al.[9] genetically labeled rat hepatocytes *in vivo* using a retrovirus harboring the β-galactosidase gene after enabling injections of the mitogen cyproterone acetate. They observed that 4% of hepatocytes were labeled, seemingly at random, and then followed the fate of these cells after retrorsine/partial hepatectomy. SHPCs occurred in clusters, and 4.6% of these clusters expressed β-galactosidase. Not unreasonably, the authors suggested that SHPCs arose at random from amongst all hepatocytes; moreover, β-galactosidase was expressed by all cells in positive clusters indicative of their clonal origin. However, biliary epithelial cells may have been labeled with the marker gene, thereby producing β-galactosidase–positive SHPC clusters from an OC response.[10] Furthermore, in a retrorsine-PH study in rats, expression of OC markers OC.2 and OC.5 was seen in a subset of SHPCs at 5 days post-PH but not at later times.[7] This transient expression of OC

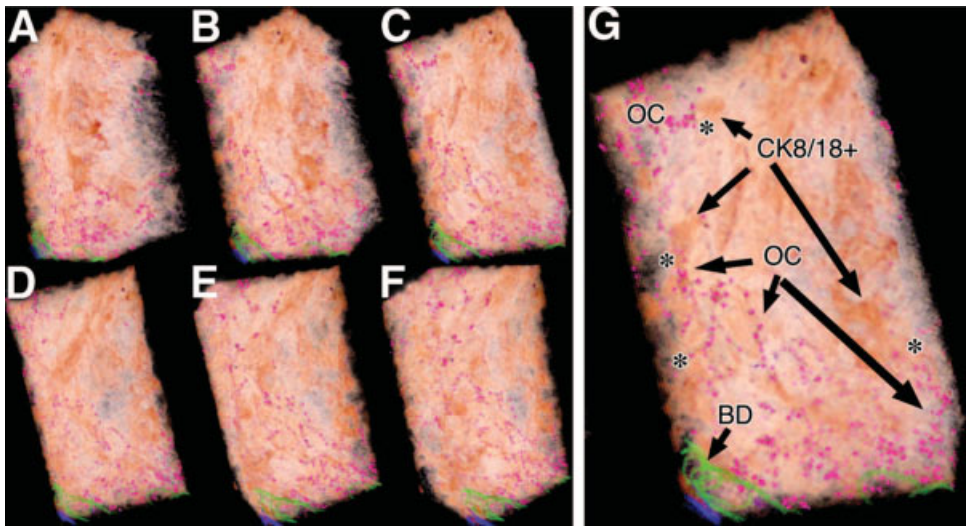

Fig. 4. Images A-F illustrates the 3-dimensional model of the nodule constructed from 100 serial sections with all tracings and original immunostained images compiled. This model is a fully manipulatable semi-transparent VRML model using the freely available 3-dimensional rendering software called FATCAM. Images A-F are being rotated to the right, showing the OCs (pink) feeding into the nodule of SHPCs from all angles shown, often terminating in CK 8/18–positive areas (darker brown areas). (G) An enlarged image demonstrating OCs penetrating the nodule and connecting directly with CK-positive areas (connections are indicated by an *), suggesting that SHPCs may originate from OCs. VRML, virtual reality modeling language; OC, oval cell; SHPC, small hepatocyte-like progenitor cells; CK, cytokeratin.

markers in SHPCs may reflect a lineage relationship of SHPCs with OCs; however, no morphological evidence for this was seen.

The 3-dimensional model constructed in this experiment shows the spatial relationship of OCs to SHPCs. Each nodule is surrounded by a prominent OC reaction. Lines of OCs penetrate the nodules directly connecting the biliary epithelia with CK 8/18–positive hepatocytes and SHPCs and some CK 8/18–negative SHPCs within the nodule. Where OCs abut SHPCs that are weakly CK8/18 positive, then an OC origin would seem likely. The significance of the low or absent CK 8/18 expression in the SHPCs is unclear; however, even the large hepatocytes without the nodules expressed CK 8/18 only weakly compared with the OCs.

Studies in mice and humans indicate that OCs also may give rise to liver tumors,[16,17] and OCs (hepatic progenitor cells) commonly surround and penetrate human liver tumors,[18-20] including those caused by hepatitis B.[21] Therefore, SHPCs could be part of a foci-nodule-carcinoma sequence of hepatocarcinogenesis.[22,23] However, in our studies, the similarity between the Ki-67 and MCM-2 labeling indices indicates the nodules are not dysplastic at the time studied. In non-dysplastic conditions, MCM-2 labeling numerically matches the Ki-67 labeling index, unlike dysplasia, in which MCM labeling far exceeds that of Ki-67.[24,25] This mouse strain typically develops hepatocellular cancer after 1 year, and analysis of later time points may clarify this. As noted in other studies of the HBsAg transgenic mouse, some of the SHPC nodules did not express HBsAg.[26] Sell[26] had preliminary evidence that cells in these foci had lost the HBsAg transgene; indeed, these HBsAg-negative foci were albumin-positive, indicating that lack of the appropriate promoter was not the reason for transgene silencing.

Several notable differences occur between a typical OC reaction and the SHPC response. In rats, OCs arise from the smallest branches of the intrahepatic biliary tree, migrate centrifugally in lines from the portal areas, and cells intermediate between OCs and hepatocytes are seen during the differentiation process. Conversely, rat SHPCs already most closely resemble hepatocytes as early as 5 days after PH in retrorsine-treated animals[7] and can form round nodules in the hepatic lobules that eventually coalesce to establish a regenerated liver indistinguishable from one generated by mature hepatocyte regeneration. Unlike the current study, SHPCs in the rat retrorsine/PH model do not seem to be physically linked with OCs.[7]

In conclusion, this study has shown minimal BM engraftment and hepatocyte transdifferentiation in a murine model of chronic liver injury. OCs and SHPCs were derived from within the liver and not from the BM. Using 3-dimensinoal image analysis of nodules, we have found that OC reactions invariably surround nodules of SHPCs and at multiple levels penetrate the nodules. These lines of intensely CK 8/18-positive OCs directly connect the portal tracts with the CK-positive SHPCs within the nodules. These weakly CK-positive SHPCs therefore appear to be of OC origin, and they intermingle with CK 8/18–negative SHPCs. Whether these CK-negative cells are of OC origin cannot be proved in this study. We therefore propose that nodules of SHPCs are at least in part of OC origin after chronic liver damage, a proposal that could be tested in future studies using the specific genetic labeling of OCs.

References

1. Evarts RP, Nagy P, Marsden E, Thorgeirsson SS. A precursor-product relationship exists between oval cells and hepatocytes in rat liver. Carcinogenesis 1987;8:1737-1740.
2. Theise ND, Badve S, Saxena R, Henegariu O, Sell S, Crawford JM, et al. Derivation of hepatocytes from bone marrow cells in mice after radiation-induced myeloablation. HEPATOLOGY 2000;31:235-240.
3. Kanazawa Y, Verma IM. Little evidence of bone marrow-derived hepatocytes in the replacement of injured liver. Proc Natl Acad Sci U S A 2003; 100(Suppl 1):11850-11853.
4. Willenbring H, Bailey AS, Foster M, Akkari Y, Dorrell C, Olson S, et al. Myelomonocytic cells are sufficient for therapeutic cell fusion in liver. Nat Med 2004;10:744-748.
5. Harris RG, Herzog EL, Bruscia EM, Grove JE, Van Arnam JS, Krause DS. Lack of a fusion requirement for development of bone marrow-derived epithelia. Science 2004;305:90-93.
6. Jang YY, Collector MI, Baylin SB, Diehl AM, Sharkis SJ. Hematopoietic stem cells convert into liver cells within days without fusion. Nat Cell Biol 2004;6:532-539.
7. Gordon GJ, Coleman WB, Hixson DC, Grisham JW. Liver regeneration in rats with retrorsine-induced hepatocellular injury proceeds through a novel cellular response. Am J Pathol 2000;156:607-619.
8. Gordon GJ, Coleman WB, Grisham JW. Temporal analysis of hepatocyte differentiation by small hepatocyte-like progenitor cells during liver regeneration in retrorsine-exposed rats. Am J Pathol 2000;157:771-786.
9. Avril A, Pichard V, Bralet MP, Ferry N. Mature hepatocytes are the source of small hepatocyte-like progenitor cells in the retrorsine model of liver injury. J Hepatol 2004;41:737-743.
10. Coleman WB, Best DH. Cellular responses in experimental liver injury: possible cellular origins of regenerative stem-like progenitor cells. HEPATOLOGY 2005;41:1173-1176.
11. Chisari FV, Pinkert CA, Milich DR, Filippi P, McLachlan A, Palmiter RD, et al. A transgenic mouse model of the chronic hepatitis B surface antigen carrier state. Science 1985;230:1157-1160.
12. Laconi S, Curreli F, Diana S, Pasciu D, De FG, Sarma DS, et al. Liver regeneration in response to partial hepatectomy in rats treated with retrorsine: a kinetic study. J Hepatol 1999;31:1069-1074.
13. Tadrous PJ. Autoreg version 2.61, 2004, and FATCAM image processing software, Version 1.03 alpha, 2003. http://www.bialith.com. 2005.
14. Alison MR, Vig P, Russo F, Bigger BW, Amofah E, Themis M, et al. Hepatic stem cells: from inside and outside the liver? Cell Prolif 2004;37: 1-21.
15. Hatch HM, Zheng D, Jorgensen ML, Petersen BE. SDF-1alpha/CXCR4: a mechanism for hepatic oval cell activation and bone marrow stem cell recruitment to the injured liver of rats. Cloning Stem Cells 2002;4:339-351.
16. Dumble ML, Croager EJ, Yeoh GC, Quail EA. Generation and characterization of p53 null transformed hepatic progenitor cells: oval cells give rise to hepatocellular carcinoma. Carcinogenesis 2002;23:435-445.

17. Roskams T, Yang SQ, Koteish A, Durnez A, DeVos R, Huang X, et al. Oxidative stress and oval cell accumulation in mice and humans with alcoholic and nonalcoholic fatty liver disease. Am J Pathol 2003;63:1301-1311.
18. Roskams T, De VR, Desmet V. 'Undifferentiated progenitor cells' in focal nodular hyperplasia of the liver. Histopathology 1996;28:291-299.
19. Libbrecht L, De VR, Cassiman D, Desmet V, Aerts R, Roskams T. Hepatic progenitor cells in hepatocellular adenomas. Am J Surg Pathol 2001; 25:1388-1396.
20. Libbrecht L, Roskams T. Hepatic progenitor cells in human liver diseases. Semin Cell Dev Biol 2002;13:389-396.
21. Lee ES, Han EM, Kim YS, Shin BK, Kim CH, Kim HK, et al. Occurrence of c-kit+ tumor cells in hepatitis B virus-associated hepatocellular carcinoma. Am J Clin Pathol 2005;124:1-6.
22. Sell S. The role of determined stem-cells in the cellular lineage of hepatocellular carcinoma. Int J Dev Biol 1993;37:189-201.
23. Sell S, Dunsford HA. Evidence for the stem cell origin of hepatocellular carcinoma and cholangiocarcinoma. Am J Pathol 1989;134:1347-1363.
24. Freeman A, Morris LS, Mills AD, Stoeber K, Laskey RA, Williams GH, et al. Minichromosome maintenance proteins as biological markers of dysplasia and malignancy. Clin Cancer Res 1999;5:2121-2132.
25. Freeman A, Hamid S, Morris L, Vowler S, Rushbrook S, Wight DG, et al. Improved detection of hepatocyte proliferation using antibody to the prereplication complex: an association with hepatic fibrosis and viral replication in chronic hepatitis C virus infection. J Viral Hepatol 2003;10:345-350.
26. Sell S. Mouse models to study the interaction of risk factors for human liver cancer. Cancer Res 2003;63:7553-7562.